Power Characteristics and Cavity Formation in Aerated Agitations

ALI FASYA ISMAIL, YOICHI NAGASE, AND JUN IMON

Department of Chemical Engineering, Hiroshima University, Higashi-Hiroshima 724, Japan

Among much of the experimental works concerning aerated agitation operation, so called "cavity concept" proposed by Bruijn et al. (1974) and Van't Riet et al. (1973, 1976) presents a way to analyze the nature of the gas dispersion around the impeller blade. The concept is quite relevant in view of the momentum transfer from impeller to fluid which was solved experimentally for single-phase agitation (Nagase et al., 1974, 1977).

The purpose of this paper is to confirm and to give reasonable prediction of the cavity structures in relation to the power characteristics through the wide range of the experimental conditions. It is also to confirm dependency of the power and cavity characteristics of operating factors. Aeration number $N_a \equiv Q_a/nd^3$, for example, has been believed to be an unique parameter in the aerated agitations in most of the previous works. But it can be unreliable that Q_a and n must cause similar effects in gas dispersion as well as power consumption.

EXPERIMENTAL

The vessel was 0.4 m in diameter and equipped with four vertical baffles at vessel wall, 0.04 m in width. Gas-free liquid depth was equal to the vessel diameter. Air was introduced through a ring sparger. The number of sparger holes and hole diameter were varied depending on the air flow rate to be a constant gas velocity through the hole. Four disc turbine impellers of different size and of number of blades were used, Table 1. The impeller position was one-third of the vessel diameter above the vessel bottom. The impeller rotational speed has been controlled within a region where air was not entrained from the liquid surface.

Photographic observations to record the gas dispersion were made through the bottom view but slightly inclined to observe the phenomena stereoscopically. Details of equipment construction are given by Ismail (1981).

EXPERIMENAL RESULTS AND DISCUSSION

Cavity Structure

To analyze air dispersion process in an aerated agitation, it is convenient to arrange the data on power measurements as a function of the impeller rotational velocity at constant air flow rate to a given impeller, Figure 1. The figure shows rather drastic variation of the relative power with the rotation speed and is classified, in general, into following four states: Flooding, Unstable Large Cavity, Large and Clinging Cavity, and Vortex Cavity.

Flooding. At very low impeller speeds, the air stream formed large bubbles at the sparger holes or on the lower surface of the impeller disc, but was not dispersed by the impeller blades. Large bubbles, thus formed, passed radially between the blades and left the disc from its edge. The situation corresponds to the flooding condition defined by Rushton and Bimbinet (1968) and Oldshue (1969). A rigid definition of this region is shown on the lefthand side of Figure 1 as the first minimum along the AA′ line where the rotational velocity, giving minimum P_g/P_o depended on the air inlet rate.

Correspondence concerning this paper should be addressed to Y. Nagase.

At the rotational speed slightly over the first minimum, some of the bubbles entered into the rear part of the inner edge of the impeller blade. With this, the relative power consumption P_g/P_o increased abruptly up to the first maximum along the BB's line. As sparging progressed, almost all the bubbles entered the rear part of the impeller blades at $n = n_{c1}$. Sparging and initial dispersion caused abrupt increases in gas holdup in the vessel, Figure 2. Dotted line shows the observed n_{c1} in the power measurement. Thus, a convenient definition for the flooding region is obtained from the holdup measurements to be $n < n_{c1}$ for a given air inlet rate.

TABLE 1. IMPELLER DIMENSIONS

No.	d (cm)	i (cm)	b (cm)	n_p (−)	Keys for Figures 3 and 4
1	11	6.4	2.3	8	△
2	16	8	3.2	6	◇
3	16	8	4	8	□
4	20	10	4	12	○

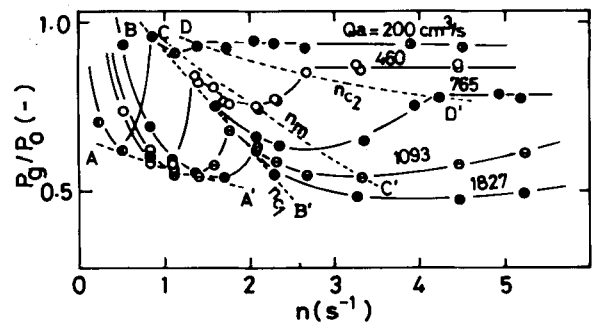

Figure 1. Power consumption as a multiple function of impeller speed; impeller No. 3.

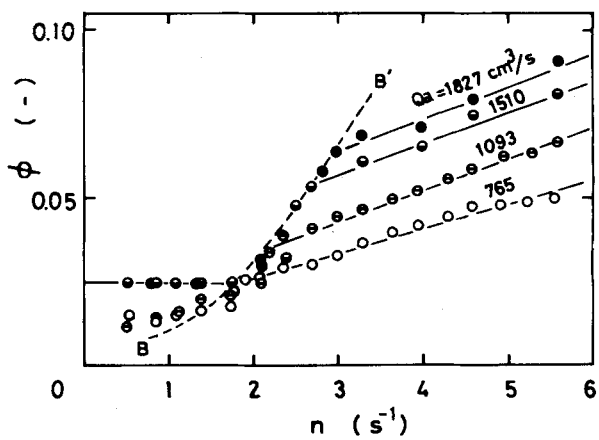

Figure 2. Holdup at constant air inlet rate; impeller No. 2.

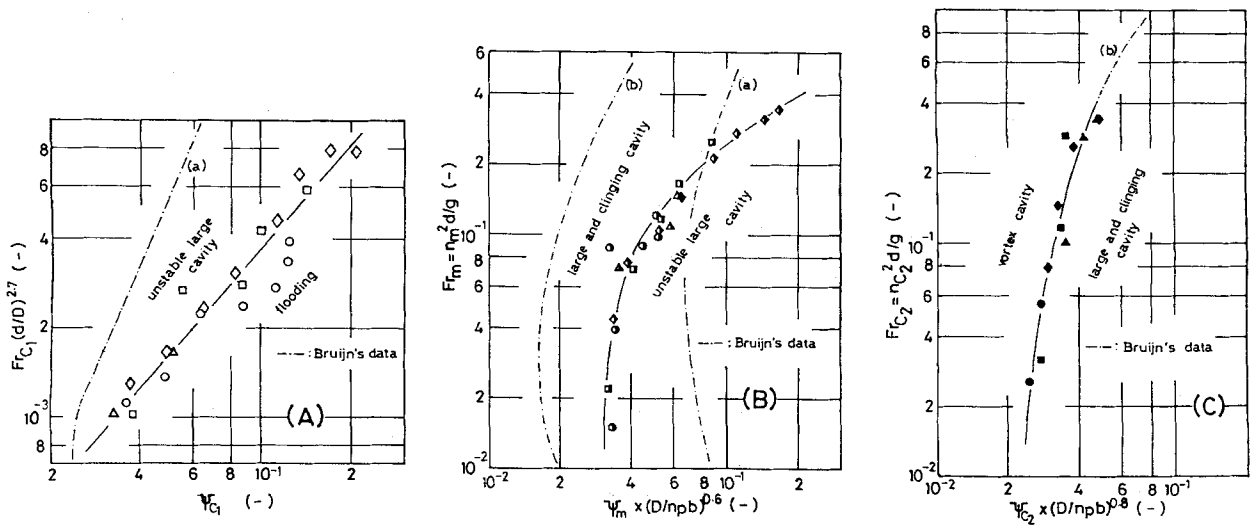

Figure 3. Correlation of critical rotation velocity with four impellers.

Unstable Large Cavity. Significant dispersion of gas took place at the impeller speeds larger than n_{c1}. Sparged gas at the rear of the impeller blade was extended radially along the blade over the whole of the blade width. For some blades, the gas film was produced from the inside blade edge to the blade tip and was then elongated into the liquid to be dispersed into smaller bubbles. The phenomenon is quite similar to that of the large cavity (Bruijn et al., 1974). Large cavities were not observed on other blades at this time. The cluster of bubbles left the blades at a midway point between the tip and the inner edge of the blade. The situation was not steady since the large cavity and cluster type cavity replaced each other with time on the same blade. Large cavities were observed for almost all the blades at $n = n_m$ which is indicated as CC′ line in Figure 1.

The relative power consumption in this region decreased with increasing the impeller rotational speed. The reduction was in conformity with the rate of large cavity formation and directly related the power consumption to the mixture density of gas and liquid around the blade.

Large and Clinging Cavity. It is to be noted that the large cavity formation, of course cluster type, indicated that the power input was still not enough to produce well-dispersed bubbles at given gas flow rate. As pointed out by Nagase et al. (1974), if the blade action is similar to a turbine-type impeller in single-phase liquid agitation, almost half of the fluid enters the impeller region stream over the edge to the rear of the blade and is discharged from it with more or less rigid rotation (Nagase et al., 1977). Therefore, if the blade agitated enough of the liquid even in a gas-liquid system, the gas film mentioned above would not occur and a clinging cavity should be produced (definitions by Bruijn et al, 1974).

Therefore, the next state, following the unstable large cavity region specified, was a competition between large and clinging cavities which corresponds to the region between CC′ and DD′ lines in Figure 1. The clinging cavities were predominantly observed with increasing the rotation velocity accompanying an increase in the relative power consumption in this region.

Vortex Cavity. At DD′ line in Figure 1, which represents the second maximum of power at $n = n_{c2}$, large cavities were not observed. A large number of small bubbles were produced from the blades. After examining the data given Bruijn et al. (1974), we concluded this region to be that of the vortex cavity type. An important result for this region was that the relative power consumptions for relatively small impellers were almost constant for a given air flow rate and that P_g/P_o with large impeller was slightly reduced with increasing the impeller speed. This corroborates the fact that the average density of gas-liquid mixture around the small impeller was almost constant within experimental conditions but density around the larger impeller was reduced with n due to the increasing ratio of recirculating bubbles into the blades.

With increasing gas inlet rate, the power curves decreased with increasing rotation velocity and do not give the same n_{c2} as well as n_{c1} and n_m. The situation can be understood since this is in the direction of flooding over the whole experimental region of the impeller rotational speeds studied.

Correlation of Critical Rotational Velocity

Figure 1 demonstrates that P_g/P_o depends simply on V_s but not on the impeller speed since multivalues of n correspond to a fixed value of P_g/P_o. Hence, the power ratio is not a single value function of the aeration number N_a.

From above discussion, the power ratio depended mainly on the density ratio of the two-phase fluid to the liquid and hence holdup, ϕ, of the cavity region.

This holdup can be defined as Eq. 1.

$$Q_a = \gamma\phi(d^2 - i^2)bn_p n \tag{1}$$

where γ is volumetric correction factor.

Rearranging Eq. 1 gives Eq. 2.

$$\phi = \psi/\gamma \tag{2}$$

where

$$\psi = (Q_a/nd^3)(d/n_p b)(d^2/(d^2 - i^2))$$

ψ includes the aeration number. The parameter was useful for experimental correlations of the boundary rotational speeds n_{c1}, n_m, and n_{c2} because it included the impeller dimensions. Plots of ψ vs. Froude number are shown in Figures 3. Line a in Figure 3(A) was reproduced from n_{c1} data given by Bruijn et al. (1974). The difference between the two results is because of the difference in definitions of the flooding. They defined the line a from the observation of the pictures, and present author, from the power measurements. In Figure 3(B), our experimental data of n_m falls reasonably well in the region between lines a and b. Line b given by Bruijn et al. (1974) was defined similar to n_{c2}. This is reproduced in Figure 3(C) to show its complete coincidence with present data of n_{c2}. The region $n > n_{c2}$, estimated here, is the region of the vortex cavity mentioned earlier.

Correlation of Power Consumption

Inclinations of the bounded lines in Figure 1 decrease from BB′ to DD′. Because of this, parameters as well as their functional relations vary in every figure in Figure 3. As a result, theoretical discription of the power ratio over wide range of operating conditions can hardly be performed. A convenient but practical plot is shown in Figure 4 in which only the data at n_{c1} (blank mark), n_m

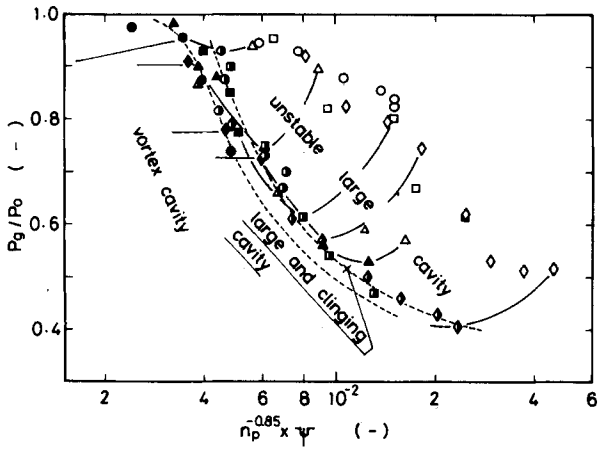

Figure 4. Power characteristics in each cavity region: black mark, at n_{c2}; half black mark, at n_m; and blank mark, at n_{c1}.

(half black mark) and n_{c2} (black mark) are plotted, and the lines illustrate where the data fall. Power ratios at n_{c1} are scattered in the figure because abscissa was chosen to be suitable for the power correlation in the large and clinging cavity region on average. All the data in this region, including those at n_m and n_{c1}, fall in a narrow area while those in Figure 1 are distributed widely depending on gas inlet rate. Data in the unstable large cavity region for given operating conditions are almost parallel to one another in the figure. The line with small inclination for the impeller No. 4 (o mark) in the vortex cavity region shows the recirculation effect of the bubbles to the impeller. The other lines in this region are almost parallel with the abscissa.

Power ratio in the large and clinging cavity region decreased discontinuously, in general, with increasing the air flow rate at constant impeller rotation as indicated by Bruijn et al. (1974). The exact boundary of this region could not be estimated from the experiments. Possible lower and higher boundaries for the region are shown on a pair of the dotted lines in Figure 4. Previous studies have used appropriate combinations of n and Q_a and usually give curves of P_g/P_o vs. N_a. Most of them cover from the vortex cavity to the large and clinging cavity and, sometimes, to the unstable large cavity region.

The procedure of power ratio estimation graphically for a given Q_a and n for a particular impeller as well as typical photographs to characterize each cavity region are given elsewhere (Ismail, 1981).

ACKNOWLEDGMENT

The authors gratefully acknowledge the editting work of G. Tatterson of Texas A&M University, College Station, TX.

NOTATION

b = impeller width
d = impeller diameter
D = tank diameter
Frc_1 = Froude number at first critical speed = $n_{c1}{}^2 d/g$
Frc_2 = Froude number at second critical speed = $n_{c2}^2 d/g$
Frm = Froude number at minimum speed = $n_m^2 d/g$
i = inside diameter of impeller blade
n = impeller rotation velocity, rps
N_a = aeration number = Q_a/nd^3
n_{c1} = impeller rotational speed on BB′ line in Figure 1
n_{c2} = impellet rotational speed on DD′ line in Figure 1
n_m = impeller rotational speed on CC′ line in Figure 1
n_p = number of impeller blades
P_g = power consumption under aeration
P_o = power consumption without aeration
Q_a = volumetric gas inlet rate
V_s = superficial gas velocity

Greek Letters

ϕ = gas holdup
ψ = nondimensional parameter defined in Eq. 2
ψ_{c1} = ψ at n_{c1}
ψ_{c2} = ψ at n_{c2}
ψ_m = ψ at n_m

LITERATURE CITED

Ismail, A. F., "Bubble Dispersion and Power Consumption in Aerated Agitation," MS Thesis, Hiroshima University, Higashi-Hiroshima, Japan (1981).

Bruijn, W., K. Van't Riet, and J. M. Smith, "Power Consumption with Aerated Rushton Turbines," *Trans. Inst. Chem. Engrs.* (London), **52**, p. 88 (1974).

Nagase, Y., and S. Sawada, "An Examination of Drag Theory Applied for Impellers in Relation to Conservation of Angular Momentum," *J. Chem. Eng. Jap.*, **10**, p. 229 (1977).

Nagase, Y., T. Yoshida, T. Iwamoto, and S. Fujita, "On Flow Characteristics in Stirred Tank with Paddle Type Impeller," *Chem. Eng.* (Japan), **38**, p. 519 (1974).

Oldshue, J. Y., "Suspending Solid and Dispersing Cases in Mixing Vessel," *Ind. Eng. Chem.*, **61**, p. 79 (1969).

Rushton, J. H., and J. J. Bimbinet, "Holdup and Flooding in Air-Liquid Mixing," *Can. J. Chem. Eng.*, **46**, p. 16 (1968).

Van't Riet, K., and J. M. Smith, "The Behaviour of Gas-Liquid Mixtures near Rushton Turbine Blade," *Chem. Eng. Sci.*, **28**, p. 1031 (1973).

Van't Riet, K., and J. M. Smith, "The Trailing Vortex System Produced by Rushton Turbine Agitators," *ibid.*, **30**, p. 1093 (1975).

Manuscript received October 7, and accepted November 15, 1982.